PERGAMON

Available online at www.sciencedirect.com
SCIENCE DIRECT®

Planetary and Space Science 50 (2002) 1117–1122

Planetary and Space Science

www.elsevier.com/locate/pss

Dynamo model with thermal convection and free-rotating inner core

I. Cupal[a], P. Hejda[a,*], M. Reshetnyak[a,b]

[a] *Geophysical Institute, Academy of Sciences of the Czech Republic, Bocni II c.p. 1401, 141 31 Prague, Czech Republic*
[b] *Institute of the Physics of the Earth, Russian Academy of Sciences, 123810 Moscow, Russia*

Received 31 May 2001; received in revised form 3 June 2002; accepted 4 June 2002

Abstract

The 2.5D approach is used to solve the dynamo model in the Boussinesq approximation. Thermal convection in a fast rotating spherical shell with a free-rotating inner core is considered. In all cases the inner core rotates slightly faster than the outer boundary of the shell. The presented dynamo model reverses regularly without any external impulse, and the generated magnetic field has the typical dipole structure at the surface. However, the dipole is aligned rather with the equatorial plane and thus the model can be applied to magnetic fields of Neptune and Uranus.

Keywords: Hydromagnetic dynamo; Thermal convection; Reversals; Inclined dipole; Inner core rotation

1. Introduction

Observations of the magnetic fields of Neptune and Uranus (Russel, 1987) indicate a magnetic dipole, which is very inclined and thus the magnetic axis is aligned rather with their equatorial plane than with their rotation axis. The kinematic study of Holme (1997) shows what features a magnetic field of this kind could have. This paper is an attempt to demonstrate such an inclined dipole in the hydromagnetic model with a free-rotating inner core powered by thermal convection.

There is little hope that we could demonstrate both rotation of the inner core and reversals in a fully 3D model using less powerful computers than Glatzmaier and Roberts (1995). On the other hand, 2D axially symmetrical models are not suitable for this investigation. Namely, the meridional velocity in axially symmetrical models is small compared to the azimuthal velocity (Anufriev and Hejda, 1999). Hence, diffusion plays the main role in the equation of heat transfer. The temperature distribution is then axially symmetrical and the azimuthal flow and the ω-effect associated with it become small. This indicates that the problem cannot be solved within the framework of axisymmetrical models. Moreover, we cannot expect the magnetic field generated in an axially symmetrical hydromagnetic dynamo model to be characterized by a very inclined dipole.

However, a 2.5D model in which just a few non-symmetrical modes are taken into account is a reasonable compromise (Jones et al., 1995). Such a 2.5D model is not as demanding on computer capability and, at the same time, does not have the drawbacks of the axisymmetrical models mentioned above. The model of the self-consistent dynamo with thermal convection is considered in the conductive outer core and the inner core is considered to have the same conductivity as the outer core. Therefore, the Lorentz force appears in the equation of motion. The inner core rotates freely, however, this rotation is additionally influenced by magnetic torque. This model of the dynamo displays some features observed in planetary magnetic fields.

The most widespread numerical method for dynamo simulations is based on the decomposition of magnetic and velocity fields into toroidal and poloidal parts and their subsequent expansion into spherical harmonics. The numerical method used in this paper deals directly with the three components of the physical fields in a spherical system of coordinates (Hejda and Reshetnyak, 1999, 2000; Hejda et al., 2001). The components are resolved in physical space for the r- and θ-coordinates and expanded into a harmonic series for the φ-coordinate. To overcome the problem of the boundary conditions for the magnetic field in the centre, all physical fields F are transformed in the manner of $f = r^{-1}F$.

* Corresponding author. Tel.: +420-2-6710-3339; fax: +420-2-7176-1549.

E-mail addresses: ic@ig.cas.cz (I. Cupal), ph@ig.cas.cz (P. Hejda), rm@uipe.srcc.msu.su (M. Reshetnyak).

URL: http://dino.scgis.ru/IPE/IPE-1/MGF/resh.htm

PII: S0032-0633(02)00051-X

2. Basic equations

Denoting $r_{\rm i}$ the inner core radius, $r_{\rm o}=L$ the outer core radius and κ the eddy thermal diffusivity, the unit of time is taken to be L^2/κ and the unit of velocity κ/L. However, we will solve the magnetohydrodynamic problem and thus it is useful to introduce L^2/η as the unit of time and η/L as the unit of velocity, where $\eta=(\mu\sigma)^{-1}$ is the magnetic diffusivity (μ is the permeability, σ the electrical conductivity). In practical calculations, we will use the Roberts number $q=\kappa/\eta=1$ and thus the "magnetic" or "non-magnetic" measures of time and velocity are practically equivalent to one another. It is then useful to choose $2\Omega\eta\rho$ for the unit of pressure p, where ρ is the density of the outer core and Ω is the rotation velocity of the spherical shell. Velocity field $\mathbf{v}$ is capable of generating magnetic field $\mathbf{B}$ in the conductive spherical shell, which can be measured in units of $\sqrt{2\Omega\eta\mu\rho}$. The problem of magnetic field generation with velocity $\mathbf{v}$ in the outer spherical shell (r,θ,φ) $(r_{\rm i}<r<r_0)$ is described by the following system of equations in the Boussinesq approximation:

$$R_{\rm o}\left(\frac{\partial\mathbf{v}}{\partial t}+\mathbf{v}\cdot\nabla\mathbf{v}\right)=-\nabla p+\mathbf{F}+E\nabla^2\mathbf{v}, \tag{1}$$

$$\frac{\partial\mathbf{B}}{\partial t}=\nabla\times(\mathbf{v}\times\mathbf{B})+\nabla^2\mathbf{B}, \tag{2}$$

$$\frac{\partial T}{\partial t}+\mathbf{v}\cdot\nabla(T+T_0)=q\nabla^2 T, \tag{3}$$

$$\nabla\cdot\mathbf{v}=0, \tag{4}$$

$$\nabla\cdot\mathbf{B}=0, \tag{5}$$

where

$$\mathbf{F}=-\mathbf{1}_z\times\mathbf{v}+qR_{\rm a}Tr\mathbf{1}_r+(\nabla\times\mathbf{B})\times\mathbf{B} \tag{6}$$

is the combined force (Coriolis, Archimedean and Lorentz). Here T is the deviation of the temperature from the prescribed temperature profile

$$T_0=\frac{r_{\rm i}/r-1}{1-r_{\rm i}},$$

where the dimensionless inner core radius is taken to be $r_{\rm i}=0.4$. The following dimensionless numbers are introduced: the Ekman number $E=\nu/(2\Omega L^2)$, the Rossby number $R_{\rm o}=\eta/(2\Omega L^2)$ and the Rayleigh number $R_{\rm a}=\alpha g_0\Theta L/2\Omega\kappa$. ν is the kinematic viscosity, α is the coefficient of volume expansion, Θ is the unit of temperature, and g_0 is the gravity acceleration at CMB $(r=r_0)$.

The system of Eqs. (1)–(6) is accompanied by non-penetrating, non-slip boundary conditions for the velocity and zero boundary conditions for temperature deviations T at ICB $(r=r_{\rm i})$ and CMB $(r=r_{\rm o})$. Vacuum boundary conditions for the magnetic field at CMB are considered. As long as the conductivity of the inner core is taken to be the same as the conductivity of the liquid outer core, no additional condition for the magnetic field at ICB is required.

In general, the inner core can rotate due to the torque of viscous and magnetic forces. The torque equation applied to the surface of the inner core reads

$$R_{\rm o}I\frac{\partial\omega}{\partial t}=2\pi r_{\rm i}^3\int_0^\pi\left[Er\frac{\partial}{\partial r}\left(\frac{\overline{v_\varphi}}{r}\right)+\overline{B_rB_\varphi}\right]_{r=r_{\rm i}}\sin^2\theta\,{\rm d}\theta, \tag{7}$$

where $I=(8/15)\pi r_{\rm i}^5$ is the moment of inertia of the inner core and the bars above certain symbols denote the average values over φ.

The so-called grid-spectral method is applied (Hejda and Reshetnyak, 1999, 2000; Hejda et al., 2001) to solve Eqs. (1)–(7). Also, this technique for a staggered grid is used in Gilman and Miller (1981). All physical fields $F(r,\theta,\varphi,t)$ are decomposed into Fourier series in terms of the azimuthal coordinate φ with coefficients that depend on time t and also on the other spherical variables (r,θ). To obtain the zero boundary conditions for the magnetic field in the centre, an additional transformation of the fields with the factor r^{-1} is used:

$$f(r,\theta,\varphi,t)=r^{-1}\sum_{m=0}^{M}F^{cm}\cos m\varphi+F^{sm}\sin m\varphi. \tag{8}$$

Eq. (8) is substituted into the system of Eqs. (1)–(7) and the system is discretized on the non-staggered (r,θ)-grid with the central second-order derivative approximation. We obtain a system of linear algebraic equations in which the second-order terms in space are treated implicitly using the Gauss–Seidel scheme. All details such as the boundary conditions in the centre of the sphere and at the axis, as well as numerous tests of magnetic field generation, can be found in Hejda and Reshetnyak (2000). Spatial time splitting (fractional step method, see, e.g., Heinrich and Pepper, 1999; Canuto et al., 1988) for the solution of the Navier–Stokes equation is also applied (Hejda et al., 2001).

3. Computer simulation

The equations of thermal convection (1), (3), (4) and (6) without the Lorentz force were tested for the critical Rayleigh numbers for the threshold of thermal convection and the free-decay mode test was also carried out. Additionally, we used the analytical solution of the free-decay modes of the Navier–Stokes equation with non-slip, non-penetrating boundary conditions to compare our numerical results to a similar stress-free case by Rheinhardt (1997). Thermal convection was studied in many previous papers (see, e.g., Busse, 1970; Busse and Finnochi, 1993), however, a free rotating core was never considered. Therefore, Eqs. (1), (3), (4), (6) and (7) were solved in orders of thermal convection, to be numerically investigated without the presence of any magnetic field. The Lorentz force and the magnetic torque were omitted in Eqs. (6) and (7), respectively. The main purpose of this "non-magnetic" approach was to find suitable convection depending on the

Ekman and Rayleigh numbers and to investigate the behaviour of the inner core rotation velocity ω. The Ekman number and Rossby numbers were chosen to be equal to one another and the Rayleigh number was decreased with decreasing Ekman (Rossby) number to keep the ratio R_a/R_o constant. This enables us to see the behaviour of the solution in which the parameters with the buoyancy, inertial and viscous terms do not change with decreasing $E = R_o$ and the amplitude of the Coriolis force increases due to increasing rotation in Eq. (6).

Although only a maximum of 4 azimuthal modes were used ($m = 0, 1, 2, 3$) with a resolution of 25 mesh points in r and θ, the obtained solution was not in contradiction with the findings of previous studies of thermal convection (see, e.g., Busse, 1970). The numerically stabilized solutions we found were quasi-periodical in all cases. The temperature distribution T within the outer core is characterized by equatorial quasi-symmetry with the typical foci of positive and negative values which appear and disappear during the quasi-period and which move in the φ-direction at the same time. The positive values of T appear more at ICB than at CMB. The changing foci in the equatorial plane are characterized by a quadrupole quasi-symmetry. The essential feature of all these solutions was that the rotation of the inner core was positive relative to the reference frame fixed to CMB.

One of the quasi-steady states of the solved thermal convection ($R_a = 320$, $E = 3.2 \times 10^{-3}$, $R_a/R_o = 10^5$, $q = 1$) was chosen as a "starter" for the solution of the fully magnetohydrodynamic problem. We used the same resolution as in the "non-magnetic" case with four wave numbers $m = 0, 1, 2, 3$. The solution oscillates, but these oscillations cannot be called quasi-periodical. The mean value of ω is slightly smaller than in the non-magnetic case, but the amplitude of its ocillations is larger and comparable to the value itself (see Fig. 1). Although the evolution of ω becomes more irregular, the rotation of the inner core remains easternly as in the non-magnetic case. The kinetic energy E_k in the magnetic case is slightly smaller than in the non-magnetic case, however, the magnetic case is characterized by the magnetic energy E_m of the same order of magnitude as the kinetic energy ($E_k \sim E_m$). This can be called the weak field regime in contrast to the usual strong field regime $E_k \ll E_m$. The snapshots of the temperature, velocity and magnetic field of this case are displayed in Figs 2–4.

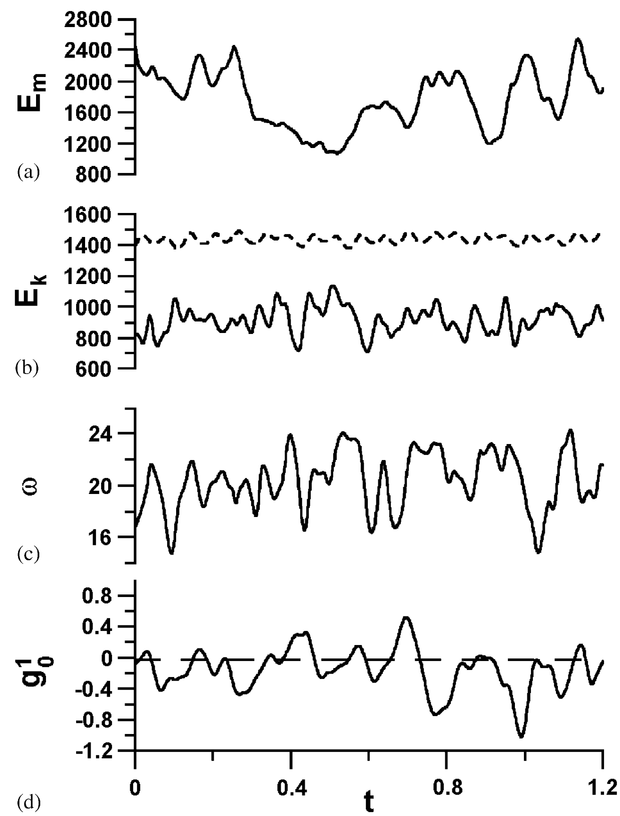

Fig. 1. Results of calculations with $R_a = 320$ and $R_o = E = 3.2 \times 10^{-3}$. Time evolution of: (a) magnetic energy $E_m \sim R_o^{-1}B^2$ of the system; (b) kinetic energy $E_k \sim v^2$ of the system (the dotted line corresponds to the non-magnetic case with the same R_a and E); (c) inner core angular velocity; (d) magnetic dipole (g_0^1 Gauss coefficient).

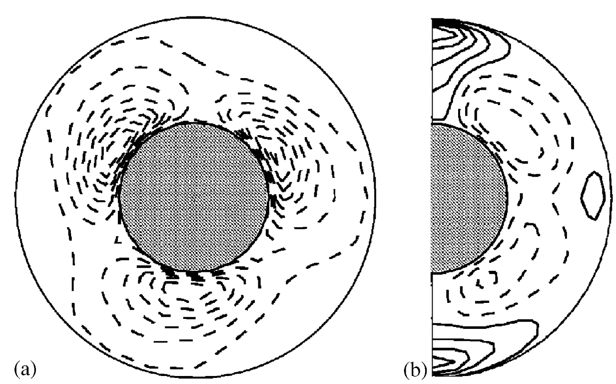

Fig. 2. The snapshots of the temperature field for $R_a = 320$ and $R_o = E = 3.2 \times 10^{-3}$. (a) equatorial section; (b) meridional section The isolines correspond to the homogeneous distribution in ranges: $(-0.9, 0.07), (-0.4, 0.5)$.

4. Applications to the planets Uranus and Neptune

Although a simple 2.5D model is not capable of modelling the subtle features of planetary magnetic fields, it can contribute to a better understanding of some global characteristics.

As mentioned in the previous section, the inner core rotation was always faster than the rotation of the mantle in all regimes considered. This fact was demonstrated for the first time by Glatzmaier and Roberts (1995) in their model of the geodynamo and verified later by seismological data (Song and Richards, 1996) for the Earth, although there still is a high degree of uncertainty in the observations of the angular velocity. In contrast to the strong field model by Glatzmaier and Roberts (1995), our model covers non-magnetic and

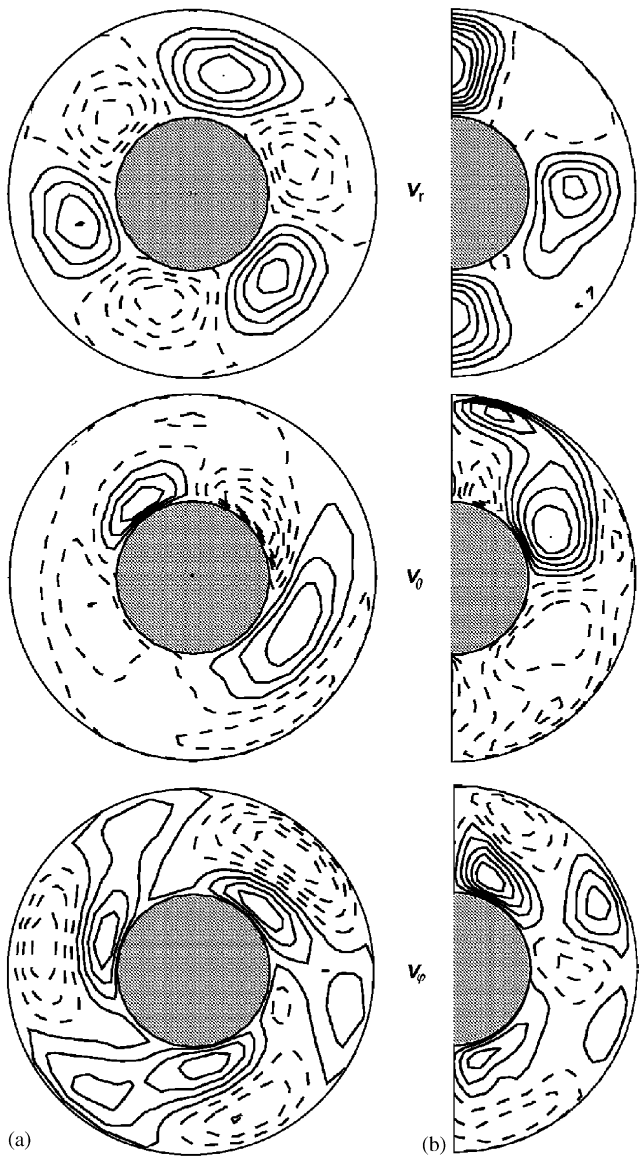

Fig. 3. The snapshots of the velocity components for $R_a = 320$ and $R_o = E = 3.2 \times 10^{-3}$. The isolines correspond to the homogeneous distribution of the presented fields in ranges: (a) equatorial section $v_r \in (-40.7, 41.3)$, $v_\theta \in (-11.0, 21.0)$, $v_\varphi \in (-50.4, 52.5)$; (b) meridional section $v_r \in (-8.9, 70.6)$, $v_\theta \in (-25.4, 46.1)$, $v_\varphi \in (-28.0, 54.3)$.

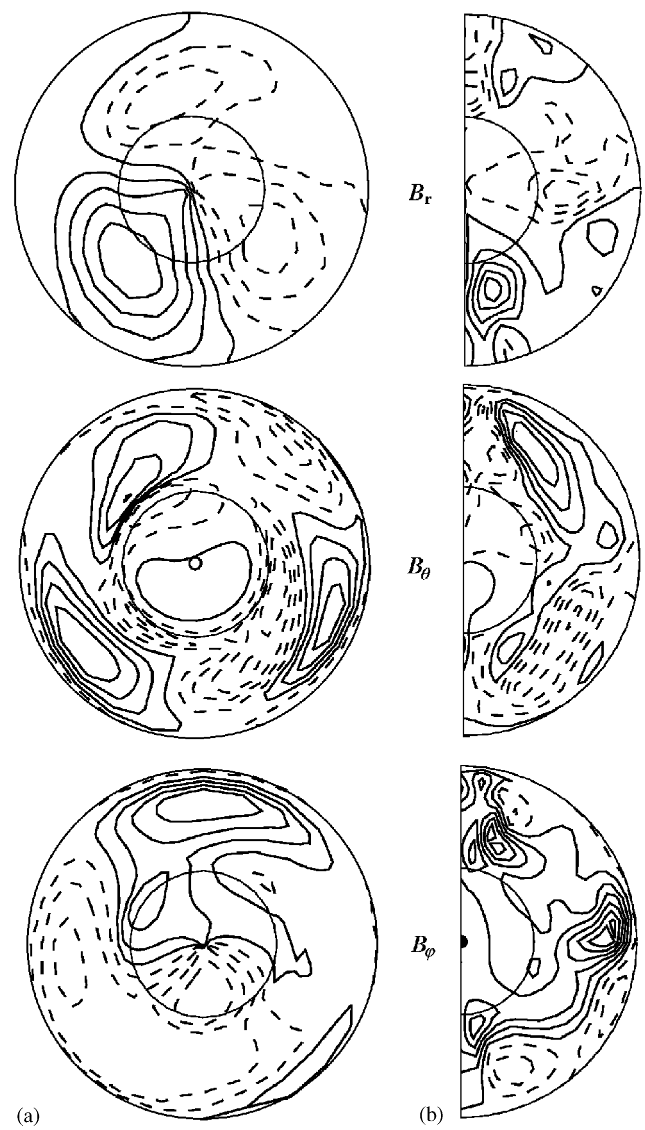

Fig. 4. The snapshots of the magnetic field components for $R_a = 320$ and $R_o = E = 3.2 \times 10^{-3}$. The isolines correspond to the homogeneous distribution of the presented fields in ranges: (a) equatorial section $B_r \in (-26.8, 52.0)$, $B_\theta \in (-9.5, 16.3)$, $B_\varphi \in (-38.8, 44.1)$; (b) meridional section $B_r \in (-23.5, 33.4)$, $B_\theta \in (-25.2, 25.8)$; $B_\varphi \in (-17.2, 44.1)$.

weak magnetic regimes of convection, Fig. 1. Thus we can say that the magnetic field has negligible influence on the direction of the inner core rotation relative to the mantle in models where viscous torque at the inner core boundary is not neglected.

One of the important characteristics of the magnetic field is the Gauss spectrum. Since the computed magnetic field varies in time, we have calculated the Gauss coefficients by integrating over the entire time interval (Fig. 5). While the ratio of the dipole to the quadrupole resembles that of the geomagnetic field, the octupole is quite larger. A deeper scrutiny of the dipole structure shows that the asymmetric dipole coefficients g_1^1, h_1^1 are larger than g_0^1, and the dipole thus lies near the equatorial plane. This means that the change of sign of coefficient g_0^1 does not represent field reversals in the sense of the geomagnetic field behaviour (from one geographical pole to the other) but just a variation of about 20° around the equator (Fig. 6).

The generation of magnetic fields with equatorial dipole symmetry became a subject of interest after Voyager II had revealed strong asymmetry in the magnetic field of Uranus. All strong planetary magnetic fields known before this discovery (Earth, Mercury, Jupiter, Saturn) were found to be dominantly dipolar with the dipole axis close to the rotation axis. The strong symmetry along the rotation axis was an "accepted paradigm" for the morphology of planetary fields. When Voyager II observed the different

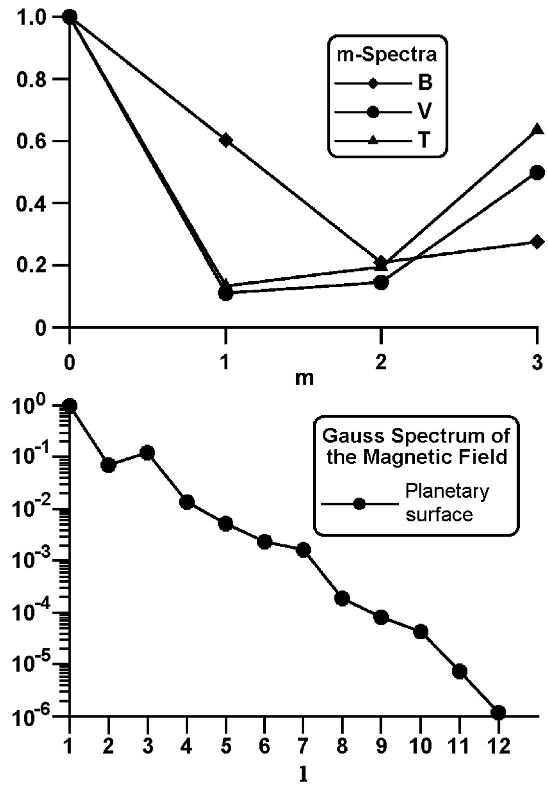

Fig. 5. M-spectrum of the fields integrated over the volume and Gauss spectrum of the magnetic field at planetary surface.

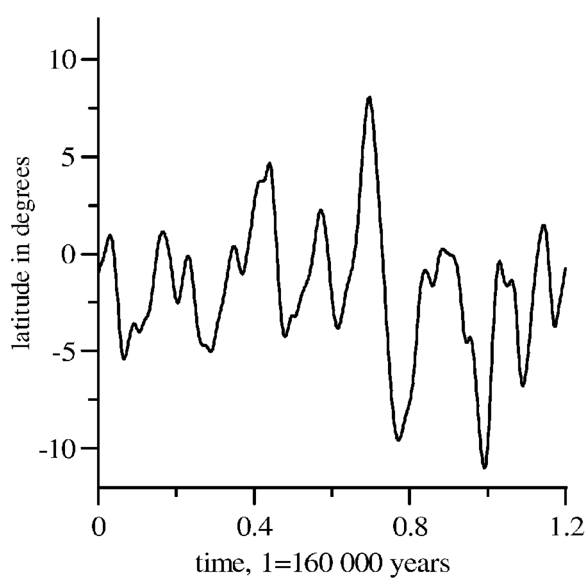

Fig. 6. Latitude dependence of the virtual dipole (Gauss coefficient g_0^1) in time.

field geometry of Uranus' magnetic field in 1986, it was speculated that the field could be just in the process of reversal (Russel, 1987), but this rather unlikely hypothesis became even less probable after the observation of a similar field structure on Neptune.

The limited collection of data (Voyager II was in the magnetosphere of Uranus for 16 h, and in that of Neptune for 38 h) could raise the question of the reliability of their interpretation. Nevertheless, a thorough analysis accomplished by Holme and Bloxham (1996) has shown that the main features described by previous models, i.e the large dipole tilts and non-dipole dominance of the field, are robust. They have estimated the dipole tilt of Uranus at 56° and of Neptune at 43°. Their analysis also suggests that the toroidal field that would be required to achieve a magnetospheric balance in the dynamo region would result in ohmic dissipation greater that the observed surface heat flow. According to their conclusions there are two possible explanations for the Uranus and Neptune field morphologies: an energetically limited dynamo and a chaotically reversing dynamo.

The first hypothesis was further studied on kinematic dynamo models by Holme (1997) and Gubbins et al. (1999). Holme (1997) found that magnetic modes with equatorial symmetry are preferred for weak differential rotation, whereas axial solutions are preferred when the toroidal velocity is dominant. Gubbins et al. (1999) investigated the general conditions for the existence of dipole/quadrupole magnetic fields with axial/equatorial symmetry. With regard to equatorial symmetry, they showed that the dipole mode is preferred for small differential rotations and meridional circulation. No equatorial quadrupole solutions were found. Holme (1997) also showed that the symmetry of the magnetic field was not influenced by the presence or absence of the inner core and that there was a small difference between conducting and insulating inner cores. On the other hand, the solution was found to be highly sensitive to the radial dependence of the flow.

Holme (1997) ends his paper with the question whether the kinematic model can be used to provide insight into the dynamical problems. Our hydromagnetic calculations give a positive answer. Looking at Fig. 3, one can see that all velocity components are of the same order of magnitude. The radial component is comparable to the other velocity components and thus there is no preference in the toroidal velocity. The distinctly longitudinal dependence of the azimuthal velocity precludes the existence of any strong differential rotation. The solution we have obtained possesses all attributes of a weak magnetic field dynamo: the toroidal and poloidal components are of the same order and the same is true for the magnetic and kinematic energies. We have also shown that the dipole magnetic field with equatorial symmetry is dynamically sustainable for a sufficiently long period of time. Our results thus show that the existence of Uranus- and Neptune-like dynamos can be understood within the scope of weak magnetic field dynamo models.

5. Conclusions

We have demonstrated that the 2.5D approach to hydromagnetic dynamo modelling is a useful tool for a better understanding of several observed phenomena. It represents a suitable complement to the most advanced 3D models by Glatzmaier and Roberts (1996) or Kuang and Bloxham (1997), which are computationally very expensive and cannot, therefore, be used to explore the entire possible parameter space.

One issue discussed in this paper was the eastward inner core rotation. This was demonstrated for the first time by Glatzmaier and Roberts (1995) and verified later by direct seismic observations (Song and Richards, 1996); see also a recent discussion of this problem by Laske and Masters (1999), Vidale et al. (2000). The crucial point of our results is that even in non-magnetic (or weak magnetic) regimes the preferable direction of the inner core rotation is eastward. Note that in the model by Glatzmaier and Roberts (1995) the magnetic torque is dominant. The same results concerning the eastward inner core rotation were obtained from the "pure magnetic" model by Kuang and Bloxham (1997), where stress-free boundary conditions were used and, hence, no viscous torque at ICB was accepted at all.

Another important conclusion is related to the Gauss magnetic spectrum. The calculation of asymmetric Gauss coefficients revealed equatorial symmetry in the magnetic dipole. This structure was observed in the magnetic fields of Uranus and Neptune. Our results contribute to the recent discussion of the conditions under which the magnetic field with equatorial dipole symmetry can be (re)generated. We have also shown that this weak field model exhibits reversals of the magnetic field, but contrary to the Earth's case the positions of virtual poles remain close to the equatorial plane.

Acknowledgements

This work was supported by the INTAS foundation (Grant 99-00348), the Russian Foundation of Basic Research (Grant 00-05-65258) and by the Grant Agency of the Academy of Sciences of the Czech Republic (Grant A3012006).

References

Anufriev, A.P., Hejda, P., 1999. Are axially symmetrical models of dynamo adequate for modelling the geodynamo? Phys. Earth Planet. Inter. 111, 69–74.

Busse, F.H., 1970. Thermal instabilities in rapidly rotating systems. J. Fluid Mech. 44, 441–460.

Busse, F.H., Finnochi, F., 1993. The onset of thermal convection in a rotating cylindrical annulus in the presence of a magnetic field. Phys. Earth Planet. Inter. 80, 13–23.

Canuto, C., Hussini, M.Y., Quarteroni, A., Zang, T.A., 1988. Spectral methods in Fluids Dynamics. Springer, Berlin, p. 567.

Gilman, P., Miller, J., 1981. Dynamically consistent non-linear dynamos driven by convection in a rotating spherical shell. Astrophys. J. Supp. Ser. 46, 211–238.

Glatzmaier, G.A., Roberts, P.H., 1995. A three-dimension convective dynamo solution with rotating and finitely conducting inner core and mantle. Phys. Earth Planet. Inter. 91, 63–75.

Glatzmaier, G.A., Roberts, P.H., 1996. An anelastic evolutionary geodynamo simulation driven by compositional and thermal convection. Physica D 97, 81–94.

Gubbins, D., Barber, C.N., Gibbons, S., Live, J.J., 1999. Kinematic dynamo action in a sphere—II. Symmetry selection. Proc. R. Soc. London A 456, 1669–1683.

Heinrich, C.J., Pepper, D.W., 1999. Intermediate Finite Element Method. Taylor & Francis, New York, p. 585.

Hejda, P., Reshetnyak, M., 1999. A grid-spectral method of the solution of the 3D kinematic geodynamo with the inner core. Stud. Geophys. Geod. 43, 319–325.

Hejda, P., Reshetnyak, M., 2000. The grid-spectral approach to 3-D geodynamo modelling. Comput. Geosci. 26, 167–175.

Hejda, P., Cupal, I., Reshetnyak, M., 2001. On the application of grid-spectral method to the solution of geodynamo equation. In: Chossat, P., Armbruster, D., Oprea, I. (Eds.), Dynamo and Dynamics, a Mathematical Challenge, Nato Science Series, Vol. 126. Kluwer Academic Publishers, Dordrecht, pp. 181–187.

Holme, R., 1997. Three-dimensional kinematic dynamos with equatorial symmetry: application to the magnetic fields of Uranus and Neptune. Phys. Earth Planet. Inter. 102, 105–122.

Holme, R., Bloxham, J., 1996. The magnetic field of Uranus and Neptune: methods and models. J. Geophys. Res. 101, 2177–2200.

Jones, C.A., Longbottom, A.W., Hollerbach, R., 1995. A self-consistent convection driven geodynamo model, using a mean field approximation. Phys. Earth Planet. Inter. 92, 119–141.

Kuang, W., Bloxham, J., 1997. An Earth-like numerical dynamo model. Nature 389, 371–374.

Laske, G., Masters, G., 1999. Limits on differential rotation of the inner core froman analysis of the Earth's free oscillations. Nature 402, 66–69.

Rheinhardt, M., 1997. Untersuchungen kinematischer und dynamisch konsistenter Dynamomodelle in sphärischer Geometrie. Ph.D. Thesis, p. 141.

Russel, C.T., 1987. Planetary magnetism. In: Jacobs, J.A. (Ed.), Geomagnetism, Vol. 2. Academic Press, London, pp. 1–177.

Song, X., Richards, P.G., 1996. Observational evidence for differential rotation of the Earth's inner core. Nature 382, 221–224.

Vidale, J.E., Dodge, D.A., Earle, P.S., 2000. Slow differential rotation of the Earth's inner core indicated by temporal changes in scattering. Nature 405, 445–448.